C. R. Mecanique 344 (2016) 532–538

Contents lists available at ScienceDirect

Comptes Rendus Mecanique

www.sciencedirect.com

Two inhomogeneities of irregular shape with internal uniform stress fields interacting with a screw dislocation

Xu Wang [a], Peter Schiavone [b,*]

[a] School of Mechanical and Power Engineering, East China University of Science and Technology, 130 Meilong Road, Shanghai 200237, China
[b] Department of Mechanical Engineering, University of Alberta, 10-203 Donadeo Innovation Centre for Engineering, Edmonton, Alberta T6G 1H9, Canada

ARTICLE INFO

Article history:
Received 17 December 2015
Accepted 3 February 2016
Available online 24 March 2016

Keywords:
Internal uniform field
Two inhomogeneities of irregular shape
Screw dislocation
Anti-plane deformation
Complex variable methods
Conformal mapping

ABSTRACT

Using complex variable methods and conformal mapping techniques, we demonstrate rigorously that two inhomogeneities of irregular shape interacting with a screw dislocation can indeed maintain uniform internal stress distributions. Our analysis indicates that while the internal uniform stresses are independent of the existence of the screw dislocation, the shapes of the two inhomogeneities required to achieve this uniformity depend on the Burgers vector, the location of the screw dislocation, and the size of the inhomogeneities. In addition, we find that this uniformity of the internal stress field is achievable also when the two inhomogeneities interact with an arbitrary number of discrete screw dislocations in the matrix.

1. Introduction

In a series of recent papers, several authors have used various approaches to demonstrate that stress distributions inside multiple non-elliptical elastic inhomogeneities remain uniform when the surrounding elastic matrix is subjected to a uniform loading at infinity (see, for example, [1–5]). It is well known, however, that a common feature of crystalline solids is the existence of dislocations [6] and that plastic deformation in solids is closely related to dislocation dynamics (see, for example, [7–13]). It is therefore of great interest to ask whether the internal stress distributions inside multiple elastic inhomogeneities of irregular shape can maintain uniformity in the presence of a number of discrete or continuously distributed dislocations in the elastic matrix surrounding the inhomogeneities.

In this paper, we take the first step towards addressing this challenging question, by asking whether it is possible to maintain internal uniform stress inside two inhomogeneities of irregular shape when either a single or multiple screw dislocations are present in a matrix subjected to uniform anti-plane shear stresses at infinity. We propose a simple yet efficient method based on complex function theory and conformal mapping techniques to determine the shapes of the two aforementioned inhomogeneities. We emphasize that our method remains valid when an arbitrary number of screw dislocations exist in the matrix.

* Corresponding author. Tel.: +1 780 492 3638.
E-mail addresses: xuwang@ecust.edu.cn (X. Wang), p.schiavone@ualberta.ca (P. Schiavone).

http://dx.doi.org/10.1016/j.crme.2016.02.008
1631-0721/

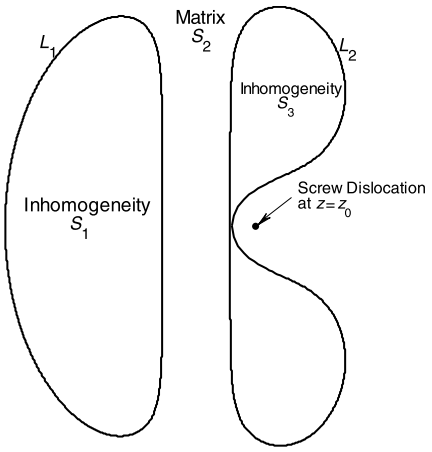

Fig. 1. Two inhomogeneities of irregular shape interacting with a screw dislocation.

2. Two inhomogeneities of irregular shape interacting with a screw dislocation

In the case of anti-plane shear deformations of an isotropic elastic material, the two shear stress components σ_{31} and σ_{32}, the out-of-plane displacement $w = u_3(x_1, x_2)$ and the associated stress function ϕ can be expressed in terms of a single analytic function $f(z)$ of the complex variable $z = x_1 + \mathrm{i}x_2$ as [14]

$$\sigma_{32} + \mathrm{i}\sigma_{31} = \mu f'(z), \quad \mu^{-1}\varphi + \mathrm{i}w = f(z) \tag{1}$$

where μ is the shear modulus of the material. The stresses σ_{31} and σ_{32} are related to the stress function φ through [14]:

$$\sigma_{31} = -\varphi_{,2}, \quad \sigma_{32} = \varphi_{,1} \tag{2}$$

Consider an infinite matrix containing two elastic inhomogeneities of irregular shape. As shown in Fig. 1, let S_1, S_2 and S_3 denote the left inhomogeneity, the matrix and the right inhomogeneity, respectively, all of which are perfectly bonded through the left and the right interfaces L_1 and L_2. The matrix is subjected to a remote uniform anti-plane shear stress field $(\sigma_{31}^{\infty}, \sigma_{32}^{\infty})$ and a single screw dislocation with Burgers vector b_3 located at $z = z_0$. In what follows, the subscripts 1, 2 and 3 (or the superscripts (1), (2) and (3)) are used to identify the associated quantities in S_1, S_2 and S_3, respectively. Our objective is to determine the shapes of the two inhomogeneities which maintain uniform internal stress distributions inside both inhomogeneities.

The continuity conditions of traction and displacement across the two interfaces L_1 and L_2 can be expressed in terms of the corresponding analytic functions in S_1, S_2 and S_3 as follows

$$\begin{aligned} &f_2(z) + \overline{f_2(z)} = \Gamma_1 f_1(z) + \Gamma_1 \overline{f_1(z)} \\ &f_2(z) - \overline{f_2(z)} = f_1(z) - \overline{f_1(z)}, \quad z \in L_1 \end{aligned} \tag{3}$$

$$\begin{aligned} &f_2(z) + \overline{f_2(z)} = \Gamma_3 f_3(z) + \Gamma_3 \overline{f_3(z)} \\ &f_2(z) - \overline{f_2(z)} = f_3(z) - \overline{f_3(z)}, \quad z \in L_2 \end{aligned} \tag{4}$$

where $\Gamma_1 = \mu_1/\mu_2$ and $\Gamma_3 = \mu_3/\mu_2$.

Adding the two conditions in Eq. (3), we obtain

$$f_2(z) = \frac{\Gamma_1 + 1}{2} f_1(z) + \frac{\Gamma_1 - 1}{2} \overline{f_1(z)}, \quad z \in L_1 \tag{5}$$

Similarly, from Eq. (4), we have

$$f_2(z) = \frac{\Gamma_3 + 1}{2} f_3(z) + \frac{\Gamma_3 - 1}{2} \overline{f_3(z)}, \quad z \in L_2 \tag{6}$$

We now construct the following conformal mapping function for the matrix:

$$\begin{aligned} &z = \omega(\xi) = R\left[\frac{1}{\xi - \lambda} + \frac{p}{\xi - \lambda^{-1}} + \frac{\Lambda^{-1}p}{\rho\xi - \lambda^{-1}} + q\log\frac{\xi - \bar{\xi}_0^{-1}}{\xi - \lambda^{-1}} + \Lambda^{-1}q\log\frac{\rho\xi - \bar{\xi}_0^{-1}}{\rho\xi - \lambda^{-1}} + \sum_{n=1}^{+\infty}\left(a_n\xi^n + a_{-n}\xi^{-n}\right)\right] \\ &\xi(z) = \omega^{-1}(z), \quad 1 \le |\xi| \le \rho^{-\frac{1}{2}} \end{aligned} \tag{7}$$

where R is a real scaling constant measuring the size of the two inhomogeneities, $\lambda(1<|\lambda|<\rho^{-\frac{1}{2}})$ and Λ are real constants, p,q and $\xi_0=\omega^{-1}(z_0)(1<|\xi_0|<\rho^{-\frac{1}{2}})$ are complex coefficients, and a_n, a_{-n} are unknown complex coefficients to be determined. The two parameters ρ and λ are variable, whilst the three parameters Λ, p, q will be obtained in the solution process presented below. In Eq. (7), the first-order pole at $\xi=\lambda$ is located within the annulus $1\le|\xi|\le\rho^{-\frac{1}{2}}$, whereas the two first-order poles at $\xi=\lambda^{-1}$ and $\xi=(\rho\lambda)^{-1}$ are both located outside the annulus. The branch cut for the logarithmic function $\log\frac{\xi-\bar{\xi}_0^{-1}}{\xi-\lambda^{-1}}$ is chosen as the line segment connecting $\xi=\bar{\xi}_0^{-1}$ and $\xi=\lambda^{-1}$ whilst that for $\log\frac{\rho\xi-\bar{\xi}_0^{-1}}{\rho\xi-\lambda^{-1}}$ is chosen as the line segment connecting $\xi=(\rho\bar{\xi}_0)^{-1}$ and $\xi=(\rho\lambda)^{-1}$. Thus the two logarithmic functions appearing in Eq. (7) are analytic, continuous and single-valued within the annulus $1\le|\xi|\le\rho^{-\frac{1}{2}}$. Using the mapping function in Eq. (7), the matrix S_2 in the z-plane is mapped onto an annulus $1\le|\xi|\le\rho^{-\frac{1}{2}}$ in the ξ-plane, while the interfaces L_1 and L_2 in the z-plane are mapped onto two co-axial circles with radii 1 and $\rho^{-\frac{1}{2}}$ in the ξ-plane, respectively. Furthermore the point at infinity ($z=\infty$) is mapped to $\xi=\lambda$. A comparison of Eq. (7) with Eq. (2) in [3] reveals the presence of additional logarithmic functions in Eq. (7) to accommodate the influence of the screw dislocation.

In order to ensure that the internal stress fields inside the two inhomogeneities are uniform, we make the following judicious choice for the functions $f_1(z)$ and $f_3(z)$

$$\begin{aligned} f_1(z)&=\frac{2k}{R(\Gamma_1+1)}z+2c_1,\quad z\in S_1\\ f_3(z)&=\frac{2k}{R(\Gamma_3+1)}z+2c_3,\quad z\in S_3 \end{aligned}\tag{8}$$

where k is a complex number to be determined and c_1 and c_3 are complex constants.

For convenience, and without loss of generality, we write $f_2(\xi)=f_2(\omega(\xi))=f_2(z)$. The following expression for $f_2(\xi)$ can be obtained from Eqs. (5), (7) and (8):

$$\begin{aligned} f_2(\xi)=k\Bigg[&\frac{1}{\xi-\lambda}+\frac{p}{\xi-\lambda^{-1}}+\frac{\Lambda^{-1}p}{\rho\xi-\lambda^{-1}}+q\log\frac{\xi-\bar{\xi}_0^{-1}}{\xi-\lambda^{-1}}+\Lambda^{-1}q\log\frac{\rho\xi-\bar{\xi}_0^{-1}}{\rho\xi-\lambda^{-1}}+\sum_{n=1}^{+\infty}\left(a_n\xi^n+a_{-n}\xi^{-n}\right)\Bigg]\\ &+\frac{\bar{k}(\Gamma_1-1)}{\Gamma_1+1}\Bigg[\frac{1}{\xi^{-1}-\lambda}+\frac{\bar{p}}{\xi^{-1}-\lambda^{-1}}+\frac{\Lambda^{-1}\bar{p}}{\rho\xi^{-1}-\lambda^{-1}}+\bar{q}\log\frac{\xi^{-1}-\xi_0^{-1}}{\xi^{-1}-\lambda^{-1}}+\Lambda^{-1}\bar{q}\log\frac{\rho\xi^{-1}-\xi_0^{-1}}{\rho\xi^{-1}-\lambda^{-1}}\\ &+\sum_{n=1}^{+\infty}\left(\bar{a}_n\xi^{-n}+\bar{a}_{-n}\xi^{n}\right)\Bigg]+c_1(\Gamma_1+1)+\bar{c}_1(\Gamma_1-1),\quad 1\le|\xi|\le\rho^{-\frac{1}{2}} \end{aligned}\tag{9}$$

We can similarly obtain a second expression for $f_2(\xi)$ from Eqs. (6)–(8):

$$\begin{aligned} f_2(\xi)=k\Bigg[&\frac{1}{\xi-\lambda}+\frac{p}{\xi-\lambda^{-1}}+\frac{\Lambda^{-1}p}{\rho\xi-\lambda^{-1}}+q\log\frac{\xi-\bar{\xi}_0^{-1}}{\xi-\lambda^{-1}}+\Lambda^{-1}q\log\frac{\rho\xi-\bar{\xi}_0^{-1}}{\rho\xi-\lambda^{-1}}+\sum_{n=1}^{+\infty}\left(a_n\xi^n+a_{-n}\xi^{-n}\right)\Bigg]\\ &+\frac{\bar{k}(\Gamma_3-1)}{\Gamma_3+1}\Bigg[\frac{1}{\rho^{-1}\xi^{-1}-\lambda}+\frac{\bar{p}}{\rho^{-1}\xi^{-1}-\lambda^{-1}}+\frac{\Lambda^{-1}\bar{p}}{\xi^{-1}-\lambda^{-1}}+\bar{q}\log\frac{\rho^{-1}\xi^{-1}-\xi_0^{-1}}{\rho^{-1}\xi^{-1}-\lambda^{-1}}\\ &+\Lambda^{-1}\bar{q}\log\frac{\xi^{-1}-\xi_0^{-1}}{\xi^{-1}-\lambda^{-1}}+\sum_{n=1}^{+\infty}\left(\bar{a}_n\rho^{-n}\xi^{-n}+\bar{a}_{-n}\rho^{n}\xi^{n}\right)\Bigg]+c_3(\Gamma_3+1)+\bar{c}_3(\Gamma_3-1),\quad 1\le|\xi|\le\rho^{-\frac{1}{2}} \end{aligned}\tag{10}$$

The compatibility of Eqs. (9) and (10) requires that Λ takes the form

$$\Lambda=\frac{(\Gamma_1+1)(\Gamma_3-1)}{(\Gamma_1-1)(\Gamma_3+1)}\tag{11}$$

and a_n and a_{-n} are given by

$$\begin{aligned} a_n&=\frac{\lambda^{-n-1}+p\Lambda^{-1}\rho^n\lambda^{n+1}+q(n\Lambda)^{-1}\rho^n(\bar{\xi}_0^n-\lambda^n)}{1-\Lambda\rho^{-n}}\\ a_{-n}&=\frac{\lambda^{n-1}+p\lambda^{1-n}-qn^{-1}(\bar{\xi}_0^{-n}-\lambda^{-n})}{\Lambda^{-1}\rho^{-n}-1},\quad n=1,2,\cdots,+\infty \end{aligned}\tag{12}$$

Additionally, from Eq. (9), the complex number k is related to the remote uniform stress field $(\sigma_{31}^{\infty},\sigma_{32}^{\infty})$ through

$$k=\frac{R(\Gamma_1+1)^2(\sigma_{32}^{\infty}+\mathrm{i}\sigma_{31}^{\infty})+R\bar{p}\lambda^2(\Gamma_1^2-1)(\sigma_{32}^{\infty}-\mathrm{i}\sigma_{31}^{\infty})}{\mu_2[(\Gamma_1+1)^2-|p|^2\lambda^4(\Gamma_1-1)^2]}\tag{13}$$

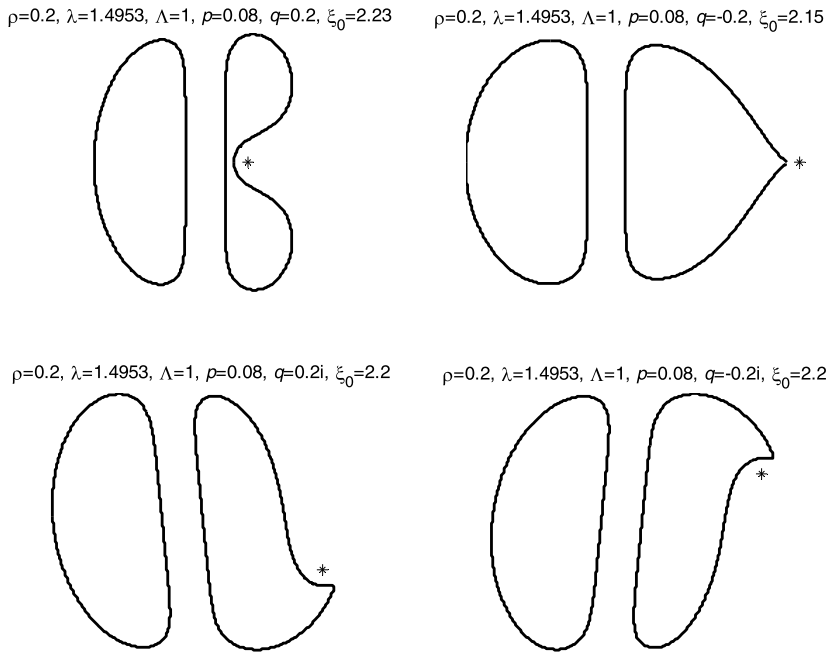

Fig. 2. The shapes of the two inhomogeneities for different values of q and ξ_0 with $\rho = 0.2, \lambda = \rho^{-\frac{1}{4}} = 1.4953, \Lambda = 1, p = 0.08$. The star in each subplot represents the location of the screw dislocation.

while the complex number q is related to the Burgers vector b_3 and the remote uniform stress field through

$$q = \frac{\mu_2 b_3[(\Gamma_1+1)^2 - |p|^2\lambda^4(\Gamma_1-1)^2]}{2\pi R[(\Gamma_1^2-1)(\sigma_{32}^{\infty} + \mathrm{i}\sigma_{31}^{\infty}) + \bar{p}\lambda^2(\Gamma_1-1)^2(\sigma_{32}^{\infty} - \mathrm{i}\sigma_{31}^{\infty})]} \tag{14}$$

Equation (14) is obtained using the fact that $f_2(\xi) \cong \frac{b_3}{2\pi}\log(\xi - \xi_0) + O(1)$ as $\xi \to \xi_0$. The expression for k in Eq. (13) implies that the values of the internal uniform stresses inside the two elastic inhomogeneities are independent of the existence of the screw dislocation. In fact, we can say that the dislocation is invisible to the two inhomogeneities as far as the internal uniform stress fields are concerned. Furthermore, since the expression for q in Eq. (14) depends on b_3 and R, the shapes of the two inhomogeneities described by $\omega(\xi)/R$ in Eq. (7) with $|\xi| = 1$ and $|\xi| = \rho^{-\frac{1}{2}}$ depend on the Burgers vector and the location of the screw dislocation as well as on the size of the two inhomogeneities.

Regarding the stresses along the two interfaces L_1 and L_2, from Eqs. (8)–(10) and (13), we can write

$$\begin{aligned}
&\left|\frac{2\Gamma_1(\sigma_{32}^{(2)} + \mathrm{i}\sigma_{31}^{(2)})}{\sigma_{32}^{(1)} + \mathrm{i}\sigma_{31}^{(1)}} - \Gamma_1 - 1\right| = |\Gamma_1 - 1|, \quad z \in L_1 \\
&\left|\frac{2\Gamma_3(\sigma_{32}^{(2)} + \mathrm{i}\sigma_{31}^{(2)})}{\sigma_{32}^{(3)} + \mathrm{i}\sigma_{31}^{(3)}} - \Gamma_3 - 1\right| = |\Gamma_3 - 1|, \quad z \in L_2
\end{aligned} \tag{15}$$

The shapes of the two inhomogeneities with internal uniform stress fields for given values of $r, \lambda, \Lambda, p, q$ and ξ_0 are illustrated in Figs. 2 and 3. We note that a careful check of the corresponding mapping functions used in identifying the shapes of the inhomogeneities in Figs. 2 and 3 reveal indeed that they are one-to-one (or conformal) for $1 \le |\xi| \le \rho^{-\frac{1}{2}}$. It is observed from Figs. 2 and 3 that the two parameters q and ξ_0, which are related to the Burgers vector, the location of the screw dislocation and the size of the two inhomogeneities, in fact exert a significant influence on the shapes of the two inhomogeneities, in particular on that of the inhomogeneity closer to the screw dislocation. Considering the definition of the parameter q in Eq. (14), we see from the second row in Figs. 2 and 3 that following a reflection about the x_1-axis for the shapes of the two inhomogeneities and the dislocation location obtained under the remote uniform loading $\sigma_{31}^{\infty} = \sigma \neq 0$ and $\sigma_{32}^{\infty} = 0$, we can obtain those corresponding to the separate remote loading $\sigma_{31}^{\infty} = -\sigma$ and $\sigma_{32}^{\infty} = 0$. We bear in mind that the Burgers vectors for the two loading cases remain the same.

We can further construct a mapping function to ensure the uniformity of internal stresses inside two inhomogeneities of irregular shape interacting with an *arbitrary number* of discrete screw dislocations in the matrix. Specifically, if we assume a total of M screw dislocations with Burgers vectors $b_3^{(j)} (j = 1, 2, \cdots, M)$ located at $z = z_j (j = 1, 2, \cdots, M)$, respectively, the corresponding mapping function is given by

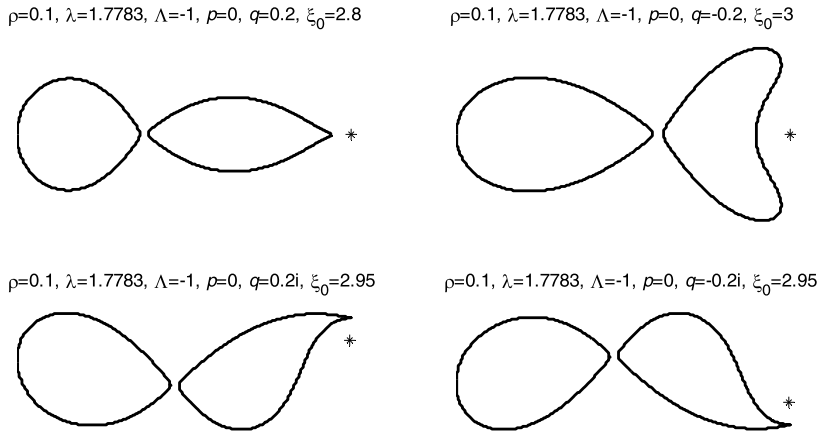

Fig. 3. The shapes of the two inhomogeneities for different values of q and ξ_0 with $\rho = 0.1, \lambda = \rho^{-\frac{1}{4}} = 1.7783, \Lambda = -1, p = 0$. The star in each subplot represents the location of the screw dislocation.

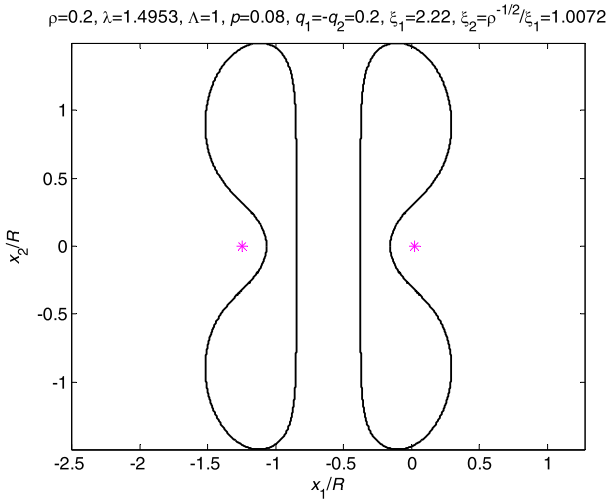

Fig. 4. The shapes of the two inhomogeneities for the parameters $\rho = 0.2, \lambda = \rho^{-\frac{1}{4}} = 1.4953, \Lambda = 1, p = 0.08, q_1 = -q_2 = 0.2, \xi_1 = 2.22, \xi_2 = \rho^{-\frac{1}{2}}/\xi_1 = 1.0072$. The two stars indicate the locations of the two screw dislocations with opposite signs.

$$z = \omega(\xi) = R\left[\frac{1}{\xi-\lambda} + \frac{p}{\xi-\lambda^{-1}} + \frac{\Lambda^{-1}p}{\rho\xi-\lambda^{-1}} + \sum_{m=1}^{M} q_m\left(\log\frac{\xi-\bar{\xi}_m^{-1}}{\xi-\lambda^{-1}} + \Lambda^{-1}\log\frac{\rho\xi-\bar{\xi}_m^{-1}}{\rho\xi-\lambda^{-1}}\right) + \sum_{n=1}^{+\infty}\left(a_n\xi^n + a_{-n}\xi^{-n}\right)\right]$$
$$\xi(z) = \omega^{-1}(z), \quad 1 \le |\xi| \le \rho^{-\frac{1}{2}} \tag{16}$$

where R and $\lambda(1 < |\lambda| < \rho^{-\frac{1}{2}})$ are real, p is complex, Λ continues to be determined by Eq. (11), $\xi_m = \omega^{-1}(z_m)$, q_m is given by

$$q_m = \frac{\mu_2 b_3^{(m)}[(\Gamma_1+1)^2 - |p|^2\lambda^4(\Gamma_1-1)^2]}{2\pi R[(\Gamma_1^2-1)(\sigma_{32}^{\infty} + \mathrm{i}\sigma_{31}^{\infty}) + \bar{p}\lambda^2(\Gamma_1-1)^2(\sigma_{32}^{\infty} - \mathrm{i}\sigma_{31}^{\infty})]} \tag{17}$$

and a_n, a_{-n} are found to be

$$a_n = \frac{\lambda^{-n-1} + p\Lambda^{-1}\rho^n\lambda^{n+1} + (n\Lambda)^{-1}\rho^n\sum_{m=1}^{M} q_m(\bar{\xi}_m^n - \lambda^n)}{1-\Lambda\rho^{-n}}$$
$$a_{-n} = \frac{\lambda^{n-1} + p\lambda^{1-n} - n^{-1}\sum_{m=1}^{M} q_m(\bar{\xi}_m^{-n} - \lambda^{-n})}{\Lambda^{-1}\rho^{-n} - 1}, \quad n = 1, 2, \cdots, +\infty \tag{18}$$

In the case of multiple screw dislocations, the internal uniform stress distributions continue to be determined by Eqs. (8) and (13) and again remain independent of the existence of the multiple screw dislocations. The stresses along the two interfaces given in Eq. (15) also remain valid in this case. We illustrate in Figs. 4–7 the shapes of the two inhomogeneities

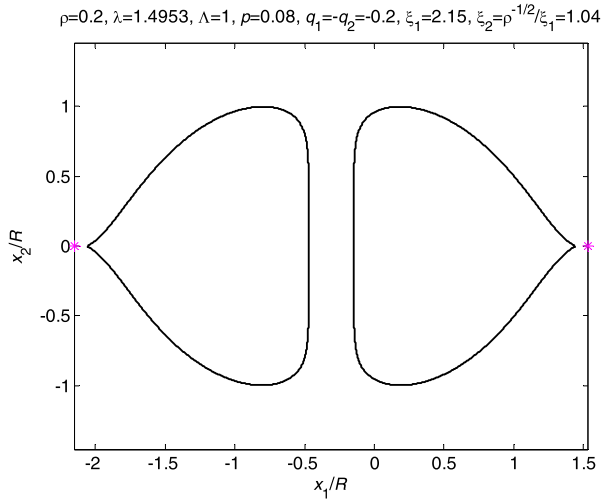

Fig. 5. The shapes of the two inhomogeneities for the parameters $\rho = 0.2, \lambda = \rho^{-\frac{1}{4}} = 1.4953, \Lambda = 1, p = 0.08, q_1 = -q_2 = -0.2, \xi_1 = 2.15, \xi_2 = \rho^{-\frac{1}{2}}/\xi_1 = 1.04$. The two stars indicate the locations of the two screw dislocations with opposite signs.

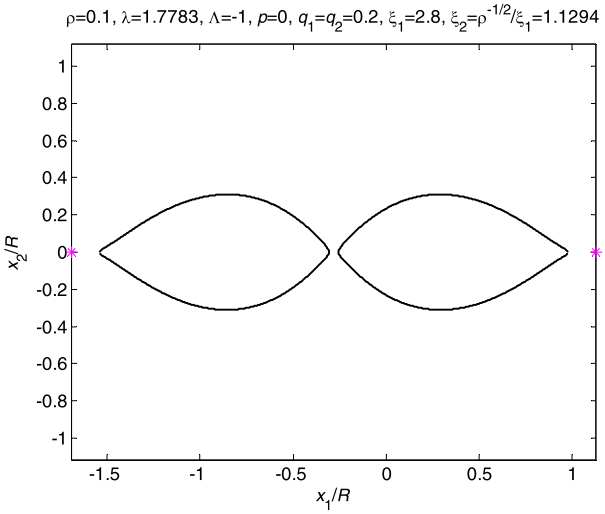

Fig. 6. The shapes of the two inhomogeneities for the parameters $\rho = 0.1, \lambda = \rho^{-\frac{1}{4}} = 1.7783, \Lambda = -1, p = 0, q_1 = q_2 = 0.2, \xi_1 = 2.8, \xi_2 = \rho^{-\frac{1}{2}}/\xi_1 = 1.1294$. The two stars indicate the locations of the two identical dislocations.

interacting with a screw dislocation dipole or with two identical dislocations. In Figs. 4 and 5, $\Lambda = 1$ (or equivalently $\Gamma_1 = \Gamma_3$) and $q_1 = -q_2$ (or equivalently $b_3^{(1)} = -b_3^{(2)}$). In Figs. 6 and 7, $\Lambda = -1$ (or equivalently $\Gamma_1\Gamma_3 = 1$) and $q_1 = q_2$ (or equivalently $b_3^{(1)} = b_3^{(2)}$). In all four figures (Figs. 4–7), the shapes of the two inhomogeneities are identical while the two screw dislocation components are distributed symmetrically with respect to the two inhomogeneity components.

3. Conclusions

We find that the uniformity property relating to stress distributions inside two inhomogeneities of irregular shape can be maintained even when the inhomogeneities interact with an arbitrary number of discrete screw dislocations located inside the surrounding matrix. The mapping functions characterizing the shapes of the two inhomogeneities are constructed in Eq. (7) for a single screw dislocation and in Eq. (16) for multiple discrete screw dislocations. Interestingly, we find that the internal uniform stress fields are independent of the existence of the single or multiple screw dislocations in the matrix. Our numerical results clearly demonstrate that the Burgers vectors and the locations of the screw dislocations, as well as the size of the two inhomogeneities play a key role in determining the shapes of the two inhomogeneities permitting internal uniform stress fields.

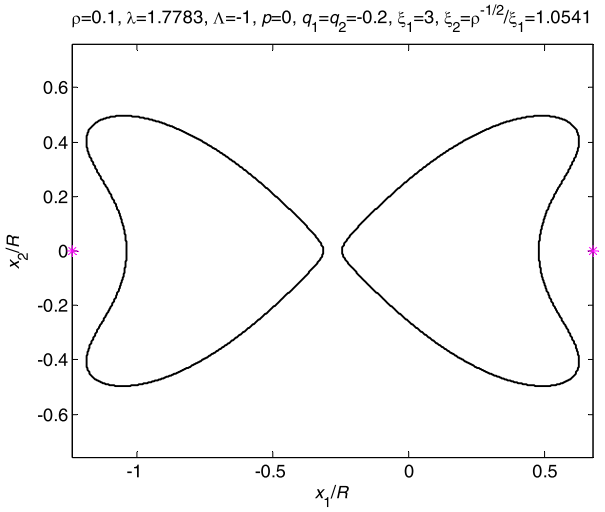

Fig. 7. The shapes of the two inhomogeneities for the parameters $\rho = 0.1, \lambda = \rho^{-\frac{1}{4}} = 1.7783, \Lambda = -1, p = 0, q_1 = q_2 = -0.2, \xi_1 = 3, \xi_2 = \rho^{-\frac{1}{2}}/\xi_1 = 1.0541$. The two stars indicate the locations of the two identical dislocations.

Acknowledgements

This work is supported by the National Natural Science Foundation of China (Grant No.: 11272121) and through a Discovery Grant from the Natural Sciences and Engineering Research Council of Canada (Grant # RGPIN 155112).

References

[1] H. Kang, E. Kim, G.W. Milton, Inclusion pairs satisfying Eshelby's uniformity property, SIAM J. Appl. Math. 69 (2008) 577–595.
[2] L.P. Liu, Solution to the Eshelby conjectures, Proc. R. Soc. A 464 (2008) 573–594.
[3] X. Wang, Uniform fields inside two non-elliptical inclusions, Math. Mech. Solids 17 (2012) 736–761.
[4] M. Dai, C.Q. Ru, C.F. Gao, Uniform strain fields inside multiple inclusions in an elastic infinite plane under anti-plane shear, Math. Mech. Solids (2014), http://dx.doi.org/10.1177/1081286514564638.
[5] M. Dai, C.Q. Ru, C.F. Gao, Uniform stress fields inside multiple inclusions in an elastic infinite plane under plane deformation, Proc. R. Soc. A 471 (2015) 20140933.
[6] G.I. Taylor, The mechanism of plastic deformation of crystals. Part I. Theoretical, Proc. R. Soc. A 145 (1934) 362–387.
[7] T. Mura, Continuous distribution of dislocations and the mathematical theory of plasticity, Phys. Status Solidi 10 (1965) 447–453.
[8] T. Mura, Continuum theory of plasticity and dislocations, Int. J. Eng. Sci. 5 (1967) 341–351.
[9] V.L. Berdichevskii, L.I. Sedov, Dynamic theory of continuously distributed dislocations. Its relation to plasticity theory, J. Appl. Math. Mech. 31 (1967) 981–1000.
[10] I. Groma, Link between the microscopic and mesoscopic length-scale description of the collective behavior of dislocations, Phys. Rev. B 56 (1997) 5807–5813.
[11] I. Groma, F.F. Csiksor, M. Zaiser, Spatial correlations and higher-order gradient terms in a continuum description of dislocation dynamics, Acta Mater. 51 (2003) 1271–1281.
[12] V. Vinogradov, J.R. Willis, The pair distribution function for an array of screw dislocations, Int. J. Solids Struct. 45 (2008) 3726–3738.
[13] V. Vinogradov, J.R. Willis, The pair distribution function for an array of screw dislocations: implications for gradient plasticity, Math. Mech. Solids 14 (2009) 161–178.
[14] T.C.T. Ting, Anisotropic Elasticity-Theory and Applications, Oxford University Press, New York, 1996.